

Data Augmentation in Temporal and Polar Domains for Event-Based Learning

HaiBo Shen, Juyu Xiao, Yihao Luo, Xiang Cao, Liangqi Zhang, Tianjiang Wang

Huazhong University of Science and Technology
 {shenhaibo, juyuxiao, luoyihao, caoxiang112, zhangliangqi, tjwang}@hust.edu.cn

Abstract

Event cameras are inherently suitable for spiking neural networks (SNNs) and have great potential in challenging scenes due to the advantages of bionics, asynchrony, high dynamic range, and no motion blur. However, novel data augmentations designed for event properties are required to process the unconventional output of these cameras in order to unlock their potential. In this paper, we explore the extraordinary influence of brightness variations due to event properties. Along the way, two novel data augmentation methods, *EventInvert* and *EventDrift* (EventID), are proposed to simulate two basic transformations of this influence. Specifically, EventID inverts or drifts events in the stream through transformations in temporal and polar domains, thereby generating samples affected by brightness variances. Extensive experiments are carried out on the CIFAR10-DVS, N-Caltech101, and N-CARS datasets. It turns out that this simulation improves generalization by increasing the robustness of models against brightness variations. In addition, EventID is broadly effective, surpassing previous state-of-the-art performances. For example, the spiking neural network model with EventID achieves a state-of-the-art accuracy of 83.50% on the CIFAR10-DVS dataset.

Introduction

Event cameras (Posch et al. 2014; Lichtsteiner, Posch, and Delbrück 2008) are bio-inspired vision sensors that operate in a completely different way from traditional cameras (Gehrig et al. 2019). Instead of capturing images at a fixed rate, the cameras asynchronously measure per-pixel brightness changes and output a stream of events that encode the time, location, and sign of the brightness changes. This bionic way of working brings attractive properties to event cameras, such as asynchrony, high dynamic range, and no motion blur. Therefore, event cameras are inherently suitable for spiking neural networks (SNNs) (Roy, Jaiswal, and Panda 2019) and have great potential in challenging computer vision scenarios (Gallego et al. 2022). To exploit this potential, an important branch of research is the event data classification (Wu et al. 2021; Zheng et al. 2021; Gu et al. 2021; Yao et al. 2021; Guo et al. 2022; Meng et al. 2022), which can provide inspiration for advanced vision tasks and a necessary foundation for exploring more biologically plausible learning rules in spiking neural networks (Li et al. 2022a; Ponghiran and Roy 2022; Chen et al. 2021).

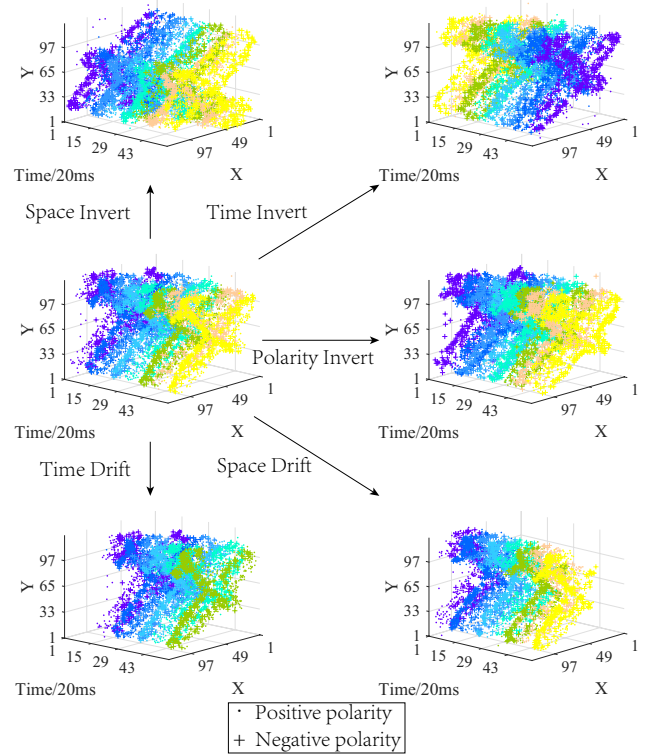


Figure 1: The examples of EventInvert and EventDrift when events are transformed in the spatial domain, temporal domain, or polar domain.

In recent years, complex neural networks have achieved significant success in classification tasks as the mainstream model (Wang et al. 2019). However, while neural networks provide strong representation capabilities, they are also easy to overfit, which weakens the generalization ability of the model (Zhong et al. 2020). As shown in Figure 3, this situation is very serious for the event data classification task and needs to be solved urgently.

A simple and efficient way to improve the generalization ability of models is data augmentation, for example, flipping (Simonyan and Zisserman 2015), translation (Shorten and Khoshgoftaar 2019), random erasing (Zhong et al.

2020). Nevertheless, due to the difference between RGB data and event data, traditional data augmentation methods are not suitable for models that learn directly from asynchronous time series event data. While these augmentation methods on RGB data can be transferred to event data through event representations (Gehrig et al. 2019; Rebecq, Horstschaefer, and Scaramuzza 2017) or frame-by-frame transformation (Li et al. 2022b), these methods generally perform unsatisfactorily in event-based learning. Because they are essentially designed for RGB data and lack the exploration of event properties.

Therefore, we reviewed the event generation model summarized in previous works (Gallego et al. 2022; Gehrig et al. 2019; Deng, Chen, and Li 2021; Gehrig et al. 2020), and found an important property of event data, that is, the influence of brightness changes on event data is significant, more so than the case in RGB data. Specifically, the event records the position, time and polarity when brightness variation (since the last event) reaches a threshold, and responds asynchronously in microseconds. Consequently, even a slight brightness variation can affect the time or polarity of events, leading to cascading changes in subsequent events. For example, a small delay at a certain moment causes an event to be generated a little later, and all events after that are delayed because they record the changes since the last event. While the RGB image synchronously respond the absolute value of brightness within milliseconds, a slight variation may not affect the current frame as long as the absolute value of total brightness does not change, so the influence of brightness variances is relatively small.

This extraordinary influence makes event data more sensitive to brightness variations, coupled with the fact that the training samples collected usually exhibit limited brightness variations, resulting in a less robust model. As mentioned above, traditional data augmentations are not designed for event data and lack the exploration of event characteristics, which are insufficient to improve this problem.

To address this problem, we analyze and conclude that inverting and drifting are the two basic ways in which brightness variations affect events, and naturally propose two novel data augmentation methods, *EventInvert* and *EventDrift* (EventID). As shown in Figure 1, EventInvert can invert events to opposite positions in temporal, spatial and polar domains, and EventDrift drifts events a certain distance in temporal or spatial domains. Essentially, EventID achieves an effect similar to traditional flipping and translation by transforming in the space domain. More importantly, EventID can simulate the influence of brightness variations on events by transforming in temporal or polar domains. Experiments show that this simulation can enhance the model robustness against brightness variations, bringing an additional significant improvement to generalization.

Our main contributions are summarized as follows:

- We analyze the reason for the extraordinary influence of brightness variations on events and conclude two basic ways that brightness variations affect events, inverting and drifting.
- We propose EventInvert and EventDrift (EventID) data

augmentations to simulate the influence of brightness variations. EventID improves the generalization of models by inverting and drifting events in spatial, temporal, and polar domains.

- Extensive experiments on N-CARS, N-Caltech101, and CIFAR10-DVS datasets demonstrate that EventID is remarkably effective and general for various event representations and network architectures. In addition, EventID brings additional improvements over naive geometric transformations by simulating the influence of brightness variations, outperforming previous SOTAs.

Related Work

Event-based Learning

Event-based learning has attracted widespread attention due to the attractive advantages of event cameras (Posch et al. 2014; Lichtsteiner, Posch, and Delbrück 2008). It can be roughly divided into two categories: one is to make full use of powerful artificial neural networks (ANNs) through event representation, which has made considerable progress in tasks such as detection and tracking (Mitrokhin et al. 2018; Cannici et al. 2019; Mondal et al. 2021), optical flow estimation (Zihao Zhu et al. 2018; Zhu et al. 2019), and image reconstruction (Paredes-Vallés and de Croon 2021; Wang, Kim, and Yoon 2020). In addition, event classification algorithms are difficult to compete with frame-based methods in static scenes, but have advantages in dynamic scenes (Gallego et al. 2022; Lee et al. 2014; Amir et al. 2017). In general, these methods rely on event representations that compress temporal or polar information, such as EventFrame (Rebecq, Horstschaefer, and Scaramuzza 2017), EventCount (Maqueda et al. 2018), VoxelGrid (Zhu et al. 2019), EST (Gehrig et al. 2019).

The other is to feed the events into the spiking neural networks (SNNs). As the third generation of neural networks, SNNs have been considered as promising models for artificial intelligence (AI) and theoretical neuroscience (Roy, Jaiswal, and Panda 2019; Zhang et al. 2022a). Intuitively, both SNNs and event cameras are bionic, asynchronous, and event-driven, so they are a natural fit. SNNs can process event streams asynchronously (Liu et al. 2020), or they can divide the event stream into many time steps (TimeSteps) according to time intervals, and then process all events sequentially (Wu et al. 2021). The main focus of SNNs is to find the most suitable biological training algorithm, so many researches focus on the simplest classification task (Zheng et al. 2021; Fang et al. 2021b; Yao et al. 2021; Li et al. 2021b; Fang et al. 2021a; Guo et al. 2022). Recently, SNNs also attempt to directly perform advanced tasks such as tracking (Zhang et al. 2022b), video reconstruction (Zhu et al. 2022, 2021), optical flow estimation (Hu et al. 2022), etc. SNNs can reach the SOTA performance with VGG9 networks (Deng et al. 2022; Meng et al. 2022), so we also use small networks when training SNNs.

Data Augmentation

The most straightforward way to alleviate overfitting is to train with more data. However, acquiring and labeling train-

ing data is costly, especially event data, since event cameras are particularly expensive. Data augmentation can effectively generate diverse data and is widely used in neural network training. The basic idea is to artificially create new samples from existing data using various transformations. For example, random flipping (Simonyan and Zisserman 2015) flips the input image horizontally or vertically to obtain a mirror image. Random cropping (Krizhevsky, Sutskever, and Hinton 2012) extracts sub-blocks from the input image to avoid the network overfitting a particular block. Translation (Shorten and Khoshgoftaar 2019) moves the image around to avoid positional biases in the data. Cutout (Devries and Taylor 2017) artificially impedes a rectangular block in the image to simulate the impact of occlusion on the image. Random erasing (Zhong et al. 2020) further optimizes the erased pixel value by adding noise. Mixup (Zhang et al. 2018) uses the weighted sum of two images as training samples to smooth the transition line between classes. In addition to traditional data augmentations, there are several event data augmentations. EventDrop (Gu et al. 2021) generates new samples by randomly removing some events through a Cutout-like operation. NDA (Li et al. 2022b) applies six traditional geometric transformations to the spatial domain of events, which can effectively enhance the generalization ability of event-based models.

The closest works to EventID are flipping, translation, and NDA (Li et al. 2022b). NDA is a collection of event geometric transformations, here mainly referring to the event versions of flipping and translation. There are several important differences between EventID and geometric transformations. Specifically, EventID considers the extraordinary influence of brightness variances and sensor noise on event data, which are ignored by flipping and translation, including the event version. EventID can transform part of events while flipping and translation can only transform the entire event stream. EventID transforms in the spatial, temporal, or polar domains while flipping and translation stay in the spatial domain. In addition, EventID can simulate samples affected by brightness variances. Experiments show that this simulation brings additional generalization improvements over naive geometric transformations.

Method

Event Generation Model

The event generation model (Gallego et al. 2022; Gehrig et al. 2019; Deng, Chen, and Li 2021; Gehrig et al. 2020) is abstracted from dynamic vision sensors (Lichtsteiner, Posch, and Delbrück 2008). Each pixel of the event camera responds to changes in its logarithmic photocurrent $L = \log(I)$. Specifically, in a noise-free scenario, an event $e_k = (x_k, y_k, t_k, p_k)$ is triggered at pixel $X_k = (y_k, x_k)$ and at time t_k as soon as the brightness variation $|\Delta L|$ reaches a temporal contrast threshold C since the last event at the pixel. The event generation model can be expressed by the following formula:

$$\Delta L(X_k, t_k) = L(X_k, t_k) - L(X_k, t_k - \Delta t_k) = p_k C \quad (1)$$

where $C > 0$, Δt_k is the time elapsed since the last event at the same pixel, and the polarity $p_k \in \{+1, -1\}$ is the sign

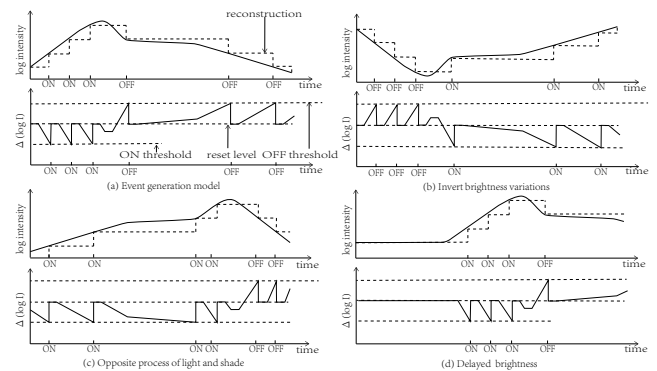


Figure 2: The relationship between logarithmic intensity and events generation for each pixel, when $|\Delta L|$ reaches the threshold, an event is generated and $|\Delta L|$ is cleared. **(a)** The event generation model, denoted as the initial brightness condition. **(b)** The way in which opposite light-dark processes affect events. **(c)** The way in which inverted brightness variations affect events. **(d)** The way in which delaying light intensity affect events.

of the brightness change. During a period, the event camera triggers events stream \mathcal{E} :

$$\mathcal{E} = \{e_k\}_{k=1}^N = \{(X_k, t_k, p_k)\}_{k=1}^N \quad (2)$$

where N represents the number of events in the set \mathcal{E} .

As shown in Figure 2 (a), an event is generated each time the brightness variances reach the threshold, and then $|\Delta L|$ is cleared. Note that due to the single-ended inverting amplifier in the sensor differential circuit, the threshold for brightness changes in the circuit is one sign different from the threshold in the conceptual model. In addition, the short segment following the firing event represents the corresponding refractory period in biological neurons and SNNs.

Further, inspired by previous work (Gehrig et al. 2019), an event field is used to represent the discrete \mathcal{E} by replacing each event of the spatiotemporal stream with a Dirac spike, resulting in a continuous representation of events. For convenience, we define the complete set of transformation domains as $D = \{X, p, t\}$, and map the polarity p from $\{-1, +1\}$ to $\{0, 1\}$. The continuous event filed S can be expressed as the following formula:

$$\begin{aligned} S(X, p, t) &= \sum_{e_k \in \mathcal{E}} \delta(X - X_k) \delta(t - t_k) \delta(p - p_k) \\ &= \sum_{e_k \in \mathcal{E}} \prod_{i \in D} \delta(i - i_k) \end{aligned} \quad (3)$$

Motivation

This work stems from observations of unusual generalizations on event data, as shown in Figure 3. When reproducing the EST (Gehrig et al. 2019) representation on three datasets, the accuracy on training samples is close to 100% but may be lower than 60% on test data. Therefore, we revisit the event generation model to find the factors that affect generalization. The influence of brightness variations catches our attention.

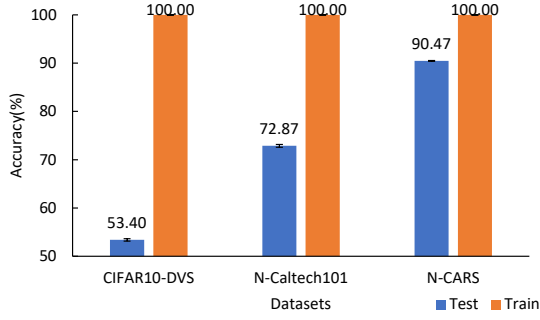


Figure 3: Poor generalization performance on event datasets.

To put it simply, the basic brightness variation scenes can be divided into three cases, the opposite light and dark change process, the inverted brightness change process, and the advance or delayed brightness change progress. As shown in Figure 2, compared to original case in Figure 2(a), the opposite light-dark change process and the inverted brightness change process in Figure 2(b, c) will invert the generated events in polar or temporal domains. The advanced or delayed brightness change progress in Figure 2(d) will drift generated events in temporal domain. These three cases are abstractions of many influencing factors, including lighting changes in real-world scenes and sensor noises.

For example, since events are easily caused by moving edges (Gallego et al. 2015, 2022), the inverted process of relative motion will cause the brightness change $|\Delta L|$ to be inverted as in Figure 2(c). Opposite light-dark progress in real-world lighting can cause $|\Delta L|$ to change as in Figure 2(b). And similarly, a delayed lighting process can lead to delayed changes in brightness as in Figure 2(d). In addition, sensor noise can also bring a similar brightness change process. For example, jitter in the step response may bring sensor delays (Lichtsteiner, Posch, and Delbrück 2008), resulting in brightness changes being delayed like Figure 2(d). The relative mismatch between the differential circuit reset level and the comparator threshold may bring a mismatch to the dynamic threshold C (Lichtsteiner, Posch, and Delbrück 2008). A short-term threshold fluctuation may lead to the advance or delayed brightness changes, similar to Figure 2(d). Therefore, these sensor noises can be regarded as a special brightness variances.

In summary, these conditions can invert or drift the temporal or polar domains of events. As a result, the basic ways in which brightness change affects events can be simplified to inverting and drifting. These observations inspired us to simulate the influence of brightness variations by generating inverted or drifted samples to improve the generalization performance of event-based learning.

EventInvert

EventInvert refers to inverting certain events \mathcal{E}_c on a specific domain d , and the transformed event field S_{ei} can be repre-

sented as:

$$S_{ei}(X, p, t) = \sum_{e_k \in \mathcal{E}_c} (\delta(d + d_k - R_d) \prod_{i \in D\{d\}} \delta(i - i_k)) \quad (4)$$

where $d \in D$, R_d represents the resolution of the domain d . When d is the time domain t , R_d represents the largest timestamp, when d is the polarity p , R_d represents 1, and when d is the space coordinate X , R_d represents the image resolution. $D\{d\}$ is the complement of d with respect to D .

EventInvert move events from d_k to their symmetrical positions $R_d - d_k$ in the event stream. As shown in Figure 1, EventInvert can invert the selected events in the time domain, spatial domain, and polarity domain, thus greatly enriching the diversity of events. When inverted in the spatial domain, it is similar to the effect of flipping frame-based images. When inverted in the temporal or polar domains, the generated samples reflect the influence of opposite brightness variations on events. The pseudocode of EventInvert is in the supplementary material.

EventDrift

EventDrift drifts events a certain distance on a specified domain, which can be represented as a convolution kernel k_{ed} :

$$k_{ed}(X, p, t) = \delta(d - r_d) \prod_{i \in D\{d\}} \delta(i) \quad (5)$$

where $d \in \{X, t\}$, r_d represents the moving distance in the domain d . The transformed event field S_{ed} can be obtained by convolving k_{ed} with the event field S :

$$\begin{aligned} S_{ed}(X, p, t) &= (k_{ed} * S)(X, p, t) \\ &= \sum_{e_k \in \mathcal{E}_c} k_{ed}(X - X_k, p - p_k, t - t_k) \\ &= \sum_{e_k \in \mathcal{E}_c} (\delta(d - d_k - r_d) \prod_{i \in D\{d\}} \delta(i - i_k)) \end{aligned} \quad (6)$$

where $d \in \{X, t\}$ and \mathcal{E}_c represents the events to be drifted.

EventDrift drifts the events a distance r in the domain d , and the part beyond borders will be discarded, as shown in Figure 1. When the samples are drifted in spatial domain, the effect of EventDrift is similar to traditional translation. In addition, drifting events in temporal domain can simulate scenarios with advanced or delayed lighting, as shown in Figure 2 (d). Note that drifted samples of different scales are generated by different distances r , which obey a uniform distribution specified by a hyperparameter. The pseudocode of EventDrift is in the supplementary material.

In addition, the event field S_{id} that applies both EventInvert and EventDrift can be obtained by convolving k_{ed} and S_{ei} :

$$S_{id}(X, p, t) = (k_{ed} * S_{ei})(X, p, t) \quad (7)$$

Experiments

In this section, we first evaluate the performance of EventInvert and EventDrift (EventID) on multiple datasets, representations, and network architectures, and compare EventID

Table 1: Performance of EventID on various representations and datasets with Resnet9 network.

Datasets	Method	Average Accuracy (Std.) (%)				
		TimeSteps (SNNs)	EventFrame	EventCount	VoxelGrid	EST
CIFAR10-DVS	Baseline	61.33(0.87)	57.00(0.49)	57.66(0.93)	55.20(0.95)	53.40(0.25)
	EventID	76.03(0.33)	78.49(0.16)	78.24(0.47)	76.71(0.54)	78.12(0.58)
N-Caltech101	Baseline	60.27(0.52)	68.52(0.35)	67.78(0.12)	71.93(0.41)	72.87(0.30)
	EventID	71.28(0.47)	72.50(0.59)	73.38(0.22)	76.87(0.15)	78.31(0.07)
N-CARS	Baseline	86.63(0.26)	91.12(0.44)	91.76(0.47)	88.71(0.26)	90.47(0.09)
	EventID	88.21(0.15)	94.04(0.29)	94.53(0.19)	93.75(0.13)	95.11(0.04)

Table 2: Performance of EventID on various architectures on N-Caltech101 dataset.

Architecture	Average Accuracy (Std.) (%)	
	Baseline	EventID
VGG7	65.06(0.24)	71.07(0.50)
Resnet9	72.87(0.30)	78.31(0.07)
Mobilenet v2	87.95(0.23)	90.74(0.28)
Resnet18	87.50(0.54)	90.58(0.59)
VGG19	87.30(0.46)	91.29(0.44)
Resnet34	90.86(0.52)	93.15(0.44)

with previous state-of-the-art models and other event data augmentation methods. Then we show more details of EventID, and experimentally demonstrate the underlying reasons for its effectiveness. Experimental results are the mean and variance of three independent runs, with the same configuration without data augmentations as the baseline.

Datasets

N-CARS dataset (Sironi et al. 2018) is recorded by an ATIS camera mounted behind the windshield. It is a large real-world event-based car classification dataset extracted from various driving courses, comprising 12,336 car samples and 11,693 non-car samples (background). The training samples include 7940 cars and 7482 backgrounds, while the test samples contain 4396 cars and 4211 backgrounds, each lasting around 100 ms.

CIFAR10-DVS dataset (Li et al. 2017) consists of 10,000 samples from CIFAR10. The recordings contain noise and blur caused by stationary DVS cameras capturing moving raw images. CIFAR10-DVS is a challenging recognition dataset due to the complexity of the samples. We follow previous work (Wu et al. 2021) and randomly select 90% of the images as training samples, and the rest are test samples for each class.

N-Caltech101 dataset (Orchard et al. 2015) is a spiking version of the original frame-based Caltech101 dataset. The Faces class has been removed from N-Caltech101 to avoid confusion, leaving 100 object classes plus a background class. The N-Caltech101 dataset is captured by mounting the ATIS sensor on a motorized pan-tilt unit and having the sen-

sor move while it views Caltech101 examples on an LCD monitor. Similarly, the ratio of training sets is 0.9.

Implementation

Various representations and architectures (Lee et al. 2020) are introduced since asynchronous event streams cannot be directly processed by neural networks, including VoxelGrid (Zhu et al. 2019), EventFrame (Rebecq, Horstschafer, and Scaramuzza 2017), EST (Gehrig et al. 2019), EventCount (Maqueda et al. 2018) for ANNs and TimeSteps (Wu et al. 2021) for SNNs. For the convenience of comparison, previous works (Wu et al. 2021; Gehrig et al. 2019; Deng et al. 2022) are reproduced as the baseline. For example, the accumulated spiking flow work (Wu et al. 2021) is regarded as the baseline of TimeSteps representation. The configurations of other experiments are the same, including a batch size of 40, an initial learning rate of $1e-4$, and an Adam (Kingma and Ba 2015) optimizer. The cross-entropy loss function is used to train the ANNs for 120 epochs, while the MSE loss function is used to train the SNNs for 50 epochs. The details of the network architectures and the detailed configurations of the experiments can be found in the supplementary material.

Broad Effectiveness

We evaluate the performance of EventID on CIFAR10-DVS, N-Caltech101, N-CARS datasets with EventFrame, EventCount, VoxelGrid, EST, TimeSteps representations, covering both ANNs and SNNs. Since the main focus of SNNs is exploring biologically plausible learning algorithms with small architectures, we uniformly adopt the Resnet9 architecture (Lee et al. 2020) in the first part of our experiments. Then we further evaluate the performance of EventID on various network architectures.

Broad Effectiveness across various representations and various datasets Extensive experiments are carried out to evaluate the broad effectiveness of the proposed method. As shown in Table 1, EventID consistently improves the performance of the model across all three popular datasets. In addition, EventID also performs well on five common representations in SNNs and ANNs. It is worth noting that EST retains the most information and has the best overall performance among the four representations in ANNs. In the following experiments, the models of SNNs use the TimeSteps

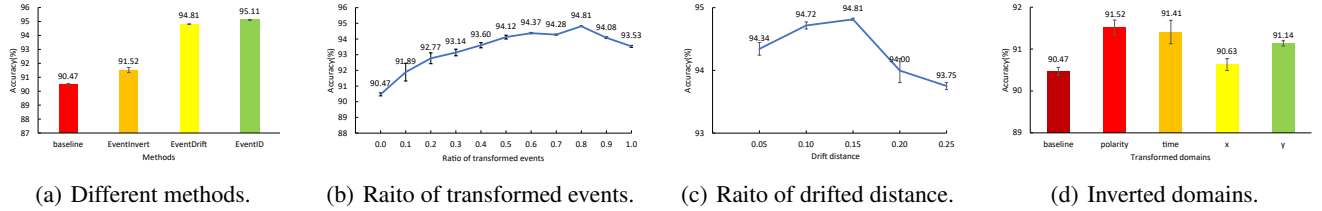


Figure 4: Performance of different hyperparameters within EventID on the N-CARS dataset with Resnet9 network.

Table 3: Performance of EventID compared to recent SOTAs on CIFAR10-DVS dataset with SNNs.

Methods	Reference	Acc.(Std.)
ASF-BP (Wu et al. 2021)	AAAI	62.50
STBP (Zheng et al. 2021)	AAAI	67.80
SEW (Fang et al. 2021a)	NeurIPS	74.40
Dspike (Li et al. 2021b)	NeurIPS	75.40(0.05)
PLIF (Fang et al. 2021b)	ICCV	74.80
TA-SNN (Yao et al. 2021)	ICCV	72.00
HR (Li et al. 2021a)	ICCV	76.80
TET (Deng et al. 2022)	ICLR	83.17(0.15)
NDA (Li et al. 2022b)	ECCV	81.70
AutoSNN (Na et al. 2022)	ICML	72.50
RecDis (Guo et al. 2022)	CVPR	72.42(0.06)
DSR (Meng et al. 2022)	CVPR	77.27(0.24)
Baseline	-	68.4(0.61)
EventID	-	83.50(0.26)

representation and the models of ANNs use the EST representation unless otherwise specified.

Broad Effectiveness across various network architectures Many powerful models in ANNs are the foundation for advanced vision tasks. To evaluate the broad effectiveness of EventID, we test the performance of EventID with multiple ANNs architectures on N-Caltech101 datasets. As shown in Table 2, EventID can significantly improve the performance of various complex models. It is worth noting that EventID achieves an accuracy of 93.15% on Resnet34.

Table 4: Performance of EventID compared with other event data augmentations on N-Caltech101 dataset, where F+T represents applying the two naive geometric transformations flipping and translation on event data.

Methods	Average Accuracy (Std.) (%)		
	VGG19 (ANNs)	Resnet34 (ANNs)	VGG9 (SNNs)
Baseline	87.30(0.46)	90.86(0.52)	66.95(0.53)
EventDrop	88.31(0.64)	92.06(0.22)	68.69(0.71)
F+T	88.84(0.73)	92.42(0.26)	77.44(0.28)
EventID	91.29(0.44)	93.15(0.44)	79.42(0.49)

Compared with Existing Methods

Compared with SOTAs As shown in Table 3, EventID can significantly improve the performance of VGG9SNN network and surpass recent state-of-the-art works. Despite the explosive progress of spiking neural networks in recent years, most of the existing work does not use data augmentation designed for event data, resulting in insufficient generalization performance. Since EventID is orthogonal to most SNN training algorithms, it can provide a better baseline and improve the performance of existing models.

Compared with Data Augmentations EventID is compared with another event data augmentation, EventDrop (Gu et al. 2021), which is similar to Cutout and achieves remarkable success on ANNs. In addition, we also migrated the traditional flipping and translation methods to the event data in a frame-by-frame manner and compared with EventID. As shown in Table 4, EventID outperforms EventDrop and geometry flipping and translation in multiple networks, covering both SNNs and ANNs. It is worth noting that the performance of EventDrop in SNNs may lag far behind EventID, as removing too many events may reduce the firing rate of SNNs, leading to "dead neurons" problem. Experiments illustrate that EventID further improves the generalization ability of the model over the basis of geometric transformations, and stably performs better.

Details of EventID

There are five important details to evaluate when implementing EventID on ANN or SNN training, including whether to apply EventInvert and EventDrift at the same time, the probability of using EventInvert and EventDrift, the suitable ratio of transformed events, the distance that EventDrift drifts, and the difference between transformations in different domains.

Performance of EventInvert and EventDrift As shown in Figure 4(a), both EventInvert and EventDrift improve the baseline. and they work better when used together. There are more comparisons between EventInvert and EventDrift in appendix. It is worth noting that drifting events is more common than inverting events, so the improvement of EventDrift is more significant.

The probability of methods As shown in Table 5, EventDrift and EventInvert perform best when the probabilities are 1 and 0.5, respectively. It is well known that a suitable degree of data augmentation is beneficial for models

Table 5: The accuracy of different transformation ratios on N-CARS dataset with Resnet9 network.

Probability	Average Accuracy (Std) (%)	
	EventDrift	EventInvert
0	90.47(0.09)	90.47(0.09)
0.25	94.16(0.08)	91.44(0.17)
0.5	94.24(0.03)	91.52(0.18)
0.75	94.37(0.19)	91.18(0.06)
1	94.81(0.02)	89.03(0.45)

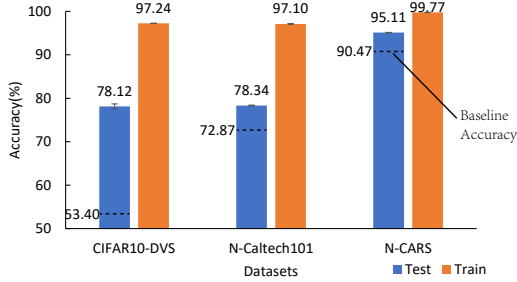


Figure 5: Generalization performance with EventID on event datasets.

to learn the feature invariance, otherwise the features may be lost or not obvious. The distance of EventDrift obeys a uniform distribution, so it is better to have a high probability. While EventInvert needs a moderate probability to keep the inverted sample and the original sample balanced.

The ratio of transformed events EventDrift is evaluated to demonstrate the performance of transformations across different ratios of events. As shown in Figure 4(b), EventDrift works best when transformed events account for 80% of all events.

The ratio of drifted distance As shown in Figure 4(c), EventDrift works best when the drift distance is 15% of the entire domain size. It also shows that the appropriate degree is important for data augmentation.

Transformations in different domain As shown in Figure 4(d), EventInvert is effective in both spatiotemporal and polar domains. It should be noted that EventInvert performs better in the polar and temporal domains, indicating that brightness variation is an essential factor affecting model generalization.

Analysis of the Effects

As shown in Figure 5, EventID significantly improves the problem of poor generalization shown in Figure 3. In addition, we also evaluate the generalization ability of EventID to unfamiliar data, and the N-Caltech101 dataset is divided into the training set, validation set, and test set with a ratio of 6:2:2. As shown in Table 6, EventID significantly improves the performance of the model on unfamiliar data, further demonstrating the generalization ability of EventID.

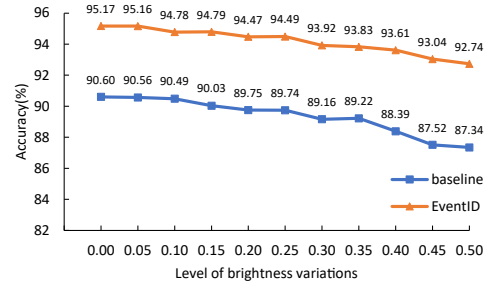


Figure 6: Performance under different levels of brightness variations on N-CARS dataset.

Table 6: Performance on the N-Caltech101 dataset with VGG19 network.

Method	Acc. No Valid.	Acc. Valid(6:2:2)
Baseline	87.30(0.46)	83.58(0.66)
EventID	91.29(0.44)	87.52(0.40)

To better understand the underlying reasons for the effectiveness of EventID, it can be seen from Table 4 that EventID significantly outperforms naive geometric flipping and translation. It shows that the transformations in the temporal and polar domains additionally improve the performance of the model, which can also be illustrated in Figure 4(d). As analyzed in the Method section, transformations in the temporal and polar domains essentially simulate the influence of brightness variances on events, so EventID is significantly effective.

To further verify that EventID indeed improves the robustness of models against brightness variations, we evaluate the performance of models by adding varying degrees of brightness perturbation to the test data. As shown in Figure 6, we take the model trained with the Resnet9 network on the N-CARS dataset and added disturbances by drifting the time of events at a ratio between 0 and 0.5. It turns out that the model with EventID generalizes significantly better under various degrees of brightness variation interference.

Extensive experiments demonstrate that by simulating the influence of brightness variations, EventID improves the robustness of models and leads to better generalization.

Conclusion

In this work, we analyze the extraordinary influence of brightness variations on events, and propose two novel event data augmentation methods: *EventInvert* and *EventDrift* (EventID). By inverting and drifting events in the temporal or polar domains, EventID simulates this influence and consequently increases the robustness of models against brightness variations. Extensive experiments demonstrate that EventID brings additional improvement over basic geometric transformations and is significantly broadly effective. In future work, we will investigate more realistic brightness variations to address the limitations of basic simulations.

References

- Amir, A.; Taba, B.; Berg, D.; Melano, T.; McKinstry, J.; Di Nolfo, C.; Nayak, T.; Andreopoulos, A.; Garreau, G.; Mendoza, M.; et al. 2017. A low power, fully event-based gesture recognition system. In *Proceedings of the IEEE conference on computer vision and pattern recognition*, 7243–7252.
- Cannici, M.; Ciccone, M.; Romanoni, A.; and Matteucci, M. 2019. Asynchronous convolutional networks for object detection in neuromorphic cameras. In *Proceedings of the IEEE/CVF Conference on Computer Vision and Pattern Recognition Workshops*, 0–0.
- Chen, Y.; Qu, H.; Zhang, M.; and Wang, Y. 2021. Deep spiking neural network with neural oscillation and spike-phase information. In *Proceedings of the AAAI Conference on Artificial Intelligence*, volume 35, 7073–7080.
- Deng, S.; Li, Y.; Zhang, S.; and Gu, S. 2022. Temporal Efficient Training of Spiking Neural Network via Gradient Reweighting. *arXiv preprint arXiv:2202.11946*.
- Deng, Y.; Chen, H.; and Li, Y. 2021. MVF-Net: A multi-view fusion network for event-based object classification. *IEEE Transactions on Circuits and Systems for Video Technology*.
- Devries, T.; and Taylor, G. W. 2017. Improved Regularization of Convolutional Neural Networks with Cutout. *CoRR*, abs/1708.04552.
- Fang, W.; Yu, Z.; Chen, Y.; Huang, T.; Masquelier, T.; and Tian, Y. 2021a. Deep residual learning in spiking neural networks. *Advances in Neural Information Processing Systems*, 34: 21056–21069.
- Fang, W.; Yu, Z.; Chen, Y.; Masquelier, T.; Huang, T.; and Tian, Y. 2021b. Incorporating learnable membrane time constant to enhance learning of spiking neural networks. In *Proceedings of the IEEE/CVF International Conference on Computer Vision*, 2661–2671.
- Gallego, G.; Delbrück, T.; Orchard, G.; Bartolozzi, C.; Taba, B.; Censi, A.; Leutenegger, S.; Davison, A. J.; Conradt, J.; Daniilidis, K.; and Scaramuzza, D. 2022. Event-Based Vision: A Survey. *IEEE Trans. Pattern Anal. Mach. Intell.*, 44(1): 154–180.
- Gallego, G.; Forster, C.; Mueggler, E.; and Scaramuzza, D. 2015. Event-based camera pose tracking using a generative event model. *arXiv preprint arXiv:1510.01972*.
- Gehrig, D.; Gehrig, M.; Hidalgo-Carrió, J.; and Scaramuzza, D. 2020. Video to events: Recycling video datasets for event cameras. In *Proceedings of the IEEE/CVF Conference on Computer Vision and Pattern Recognition*, 3586–3595.
- Gehrig, D.; Loquercio, A.; Derpanis, K. G.; and Scaramuzza, D. 2019. End-to-End Learning of Representations for Asynchronous Event-Based Data. In *2019 IEEE/CVF International Conference on Computer Vision, ICCV 2019, Seoul, Korea (South), October 27 - November 2, 2019*, 5632–5642. IEEE.
- Gu, F.; Sng, W.; Hu, X.; and Yu, F. 2021. EventDrop: Data Augmentation for Event-based Learning. In Zhou, Z., ed., *Proceedings of the Thirtieth International Joint Conference on Artificial Intelligence, IJCAI 2021, Virtual Event / Montreal, Canada, 19-27 August 2021*, 700–707. ijcai.org.
- Guo, Y.; Tong, X.; Chen, Y.; Zhang, L.; Liu, X.; Ma, Z.; and Huang, X. 2022. RecDis-SNN: Rectifying Membrane Potential Distribution for Directly Training Spiking Neural Networks. In *Proceedings of the IEEE/CVF Conference on Computer Vision and Pattern Recognition*, 326–335.
- Hu, L.; Zhao, R.; Ding, Z.; Ma, L.; Shi, B.; Xiong, R.; and Huang, T. 2022. Optical Flow Estimation for Spiking Camera. In *Proceedings of the IEEE/CVF Conference on Computer Vision and Pattern Recognition*, 17844–17853.
- Kingma, D. P.; and Ba, J. 2015. Adam: A Method for Stochastic Optimization. In Bengio, Y.; and LeCun, Y., eds., *3rd International Conference on Learning Representations, ICLR 2015, San Diego, CA, USA, May 7-9, 2015, Conference Track Proceedings*.
- Krizhevsky, A.; Sutskever, I.; and Hinton, G. E. 2012. ImageNet Classification with Deep Convolutional Neural Networks. In *NeurIPS*, volume 25.
- Lee, C.; Sarwar, S. S.; Panda, P.; and et al. 2020. Enabling Spike-Based Backpropagation for Training Deep Neural Network Architectures. *Frontiers in Neuroscience*, 14: 119.
- Lee, J. H.; Delbruck, T.; Pfeiffer, M.; Park, P. K.; Shin, C.-W.; Ryu, H.; and Kang, B. C. 2014. Real-time gesture interface based on event-driven processing from stereo silicon retinas. *IEEE transactions on neural networks and learning systems*, 25(12): 2250–2263.
- Li, H.; Liu, H.; Ji, X.; and et al. 2017. CIFAR10-DVS: An Event-Stream Dataset for Object Classification. *Frontiers in Neuroscience*, 11: 309.
- Li, S.; Feng, Y.; Li, Y.; Jiang, Y.; Zou, C.; and Gao, Y. 2021a. Event Stream Super-Resolution via Spatiotemporal Constraint Learning. In *Proceedings of the IEEE/CVF International Conference on Computer Vision*, 4480–4489.
- Li, W.; Chen, H.; Guo, J.; Zhang, Z.; and Wang, Y. 2022a. Brain-inspired multilayer perceptron with spiking neurons. In *Proceedings of the IEEE/CVF Conference on Computer Vision and Pattern Recognition*, 783–793.
- Li, Y.; Guo, Y.; Zhang, S.; Deng, S.; Hai, Y.; and Gu, S. 2021b. Differentiable spike: Rethinking gradient-descent for training spiking neural networks. *Advances in Neural Information Processing Systems*, 34: 23426–23439.
- Li, Y.; Kim, Y.; Park, H.; Geller, T.; and Panda, P. 2022b. Neuromorphic Data Augmentation for Training Spiking Neural Networks. *arXiv preprint arXiv:2203.06145*.
- Lichtsteiner, P.; Posch, C.; and Delbrück, T. 2008. A 128×128 120 dB 15 μ s Latency Asynchronous Temporal Contrast Vision Sensor. *IEEE J. Solid State Circuits*, 43(2): 566–576.
- Liu, Q.; Ruan, H.; Xing, D.; Tang, H.; and Pan, G. 2020. Effective aer object classification using segmented probability-maximization learning in spiking neural networks. In *Proceedings of the AAAI Conference on Artificial Intelligence*, volume 34, 1308–1315.
- Maqueda, A. I.; Loquercio, A.; Gallego, G.; García, N.; and Scaramuzza, D. 2018. Event-Based Vision Meets Deep

- Learning on Steering Prediction for Self-Driving Cars. In *2018 IEEE Conference on Computer Vision and Pattern Recognition, CVPR 2018, Salt Lake City, UT, USA, June 18-22, 2018*, 5419–5427. Computer Vision Foundation / IEEE Computer Society.
- Meng, Q.; Xiao, M.; Yan, S.; Wang, Y.; Lin, Z.; and Luo, Z.-Q. 2022. Training High-Performance Low-Latency Spiking Neural Networks by Differentiation on Spike Representation. In *Proceedings of the IEEE/CVF Conference on Computer Vision and Pattern Recognition*, 12444–12453.
- Mitrokhin, A.; Fermüller, C.; Parameshwara, C.; and Aloimonos, Y. 2018. Event-based moving object detection and tracking. In *2018 IEEE/RSJ International Conference on Intelligent Robots and Systems (IROS)*, 1–9. IEEE.
- Mondal, A.; Giraldo, J. H.; Bouwmans, T.; Chowdhury, A. S.; et al. 2021. Moving Object Detection for Event-based Vision using Graph Spectral Clustering. In *Proceedings of the IEEE/CVF International Conference on Computer Vision*, 876–884.
- Na, B.; Mok, J.; Park, S.; Lee, D.; Choe, H.; and Yoon, S. 2022. AutoSNN: Towards Energy-Efficient Spiking Neural Networks. *arXiv preprint arXiv:2201.12738*.
- Orchard, G.; Jayawant, A.; Cohen, G.; and Thakor, N. V. 2015. Converting Static Image Datasets to Spiking Neuro-morphic Datasets Using Saccades. *CoRR*, abs/1507.07629.
- Paredes-Vallés, F.; and de Croon, G. C. 2021. Back to event basics: Self-supervised learning of image reconstruction for event cameras via photometric constancy. In *Proceedings of the IEEE/CVF Conference on Computer Vision and Pattern Recognition*, 3446–3455.
- Ponghiran, W.; and Roy, K. 2022. Spiking Neural Networks with Improved Inherent Recurrence Dynamics for Sequential Learning. In *Proceedings of the AAAI Conference on Artificial Intelligence*, volume 36, 8001–8008.
- Posch, C.; Serrano-Gotarredona, T.; Linares-Barranco, B.; and Delbrück, T. 2014. Retinomorph Event-Based Vision Sensors: Bioinspired Cameras With Spiking Output. *Proc. IEEE*, 102(10): 1470–1484.
- Rebecq, H.; Horstschaefter, T.; and Scaramuzza, D. 2017. Real-time Visual-Inertial Odometry for Event Cameras using Keyframe-based Nonlinear Optimization. In *British Machine Vision Conference 2017, BMVC 2017, London, UK, September 4-7, 2017*. BMVA Press.
- Roy, K.; Jaiswal, A.; and Panda, P. 2019. Towards spike-based machine intelligence with neuromorphic computing. *Nature*, 575(7784): 607–617.
- Shorten, C.; and Khoshgoftaar, T. M. 2019. A survey on Image Data Augmentation for Deep Learning. *J. Big Data*.
- Simonyan, K.; and Zisserman, A. 2015. Very Deep Convolutional Networks for Large-Scale Image Recognition. In Bengio, Y.; and LeCun, Y., eds., *International Conference on Learning Representations, ICLR 2015*.
- Sironi, A.; Brambilla, M.; Bourdis, N.; Lagorce, X.; and Benosman, R. 2018. HATS: Histograms of Averaged Time Surfaces for Robust Event-Based Object Classification. In *CVPR*.
- Wang, L.; Kim, T.-K.; and Yoon, K.-J. 2020. Eventsr: From asynchronous events to image reconstruction, restoration, and super-resolution via end-to-end adversarial learning. In *Proceedings of the IEEE/CVF Conference on Computer Vision and Pattern Recognition*, 8315–8325.
- Wang, W.; Yang, Y.; Wang, X.; Wang, W.; and Li, J. 2019. Development of convolutional neural network and its application in image classification: a survey. *Optical Engineering*, 58(4): 040901.
- Wu, H.; Zhang, Y.; Weng, W.; and et al. 2021. Training Spiking Neural Networks with Accumulated Spiking Flow. *AAAI*, 35(12): 10320–10328.
- Yao, M.; Gao, H.; Zhao, G.; Wang, D.; Lin, Y.; Yang, Z.; and Li, G. 2021. Temporal-wise attention spiking neural networks for event streams classification. In *Proceedings of the IEEE/CVF International Conference on Computer Vision*, 10221–10230.
- Zhang, D.; Zhang, T.; Jia, S.; Wang, Q.; and Xu, B. 2022a. Recent Advances and New Frontiers in Spiking Neural Networks. *arXiv preprint arXiv:2204.07050*.
- Zhang, H.; Cissé, M.; Dauphin, Y. N.; and Lopez-Paz, D. 2018. mixup: Beyond Empirical Risk Minimization. In *6th International Conference on Learning Representations, ICLR 2018, Vancouver, BC, Canada, April 30 - May 3, 2018, Conference Track Proceedings*. OpenReview.net.
- Zhang, J.; Dong, B.; Zhang, H.; Ding, J.; Heide, F.; Yin, B.; and Yang, X. 2022b. Spiking Transformers for Event-Based Single Object Tracking. In *Proceedings of the IEEE/CVF Conference on Computer Vision and Pattern Recognition*, 8801–8810.
- Zheng, H.; Wu, Y.; Deng, L.; Hu, Y.; and Li, G. 2021. Going deeper with directly-trained larger spiking neural networks. In *Proceedings of the AAAI Conference on Artificial Intelligence*, 11062–11070.
- Zhong, Z.; Zheng, L.; Kang, G.; Li, S.; and Yang, Y. 2020. Random erasing data augmentation. In *Proceedings of the AAAI conference on artificial intelligence*, volume 34, 13001–13008.
- Zhu, A. Z.; Yuan, L.; Chaney, K.; and Daniilidis, K. 2019. Unsupervised Event-Based Learning of Optical Flow, Depth, and Egomotion. In *IEEE Conference on Computer Vision and Pattern Recognition, CVPR 2019, Long Beach, CA, USA, June 16-20, 2019*, 989–997. Computer Vision Foundation / IEEE.
- Zhu, L.; Li, J.; Wang, X.; Huang, T.; and Tian, Y. 2021. NeuSpike-Net: High Speed Video Reconstruction via Bio-inspired Neuromorphic Cameras. In *Proceedings of the IEEE/CVF International Conference on Computer Vision*.
- Zhu, L.; Wang, X.; Chang, Y.; Li, J.; Huang, T.; and Tian, Y. 2022. Event-based Video Reconstruction via Potential-assisted Spiking Neural Network. In *Proceedings of the IEEE/CVF Conference on Computer Vision and Pattern Recognition*, 3594–3604.
- Zihao Zhu, A.; Yuan, L.; Chaney, K.; and Daniilidis, K. 2018. Unsupervised event-based optical flow using motion compensation. In *Proceedings of the European Conference on Computer Vision (ECCV) Workshops*, 0–0.